Molecular Vision 2017; 23:922-932 <http://www.molvis.org/molvis/v23/922>
Received 20 March 2017 | Accepted 11 December 2017 | Published 13 December 2017

Possible involvement of NETosis in inflammatory processes in the eye: Evidence from a small cohort of patients

Tilda Barliya,[1] Rima Dardik,[2] Yael Nisgav,[1] Mor Dachbash,[1] Dan Gaton,[3,4] Gili Kenet,[2,4] Rita Ehrlich,[3,4] Dov Weinberger,[1,3,4] Tami Livnat[1,2,4]

(The first two authors contributed equally to this study)

[1]Laboratory of Eye research Felsenstein Medical Research Center (FMRC), Rabin Medical Center, Petah Tikva, Israel; [2]The Israeli National Hemophilia Center, Sheba Medical Center, Tel Hashomer, Israel; [3]Division of Ophthalmology, Rabin Medical Center- Beilinson campus, Petah Tikva, Israel; [4]Sackler School of Medicine, Tel-Aviv University, Israel

Purpose: To evaluate whether NETosis is involved in cytokine-induced ocular inflammation and to track neutrophil extracellular traps (NET) complexes in patients with proliferative diabetic retinopathy (PDR).
Methods: For the animal model, the eyes of C57BL/6J mice were intravitreally injected with interleukin-8 (IL-8), tumor necrosis factor alpha (TNF-α), or saline. Histology and immunofluorescence staining for CD11b, neutrophil elastase (NE), myeloperoxidase (MPO), citrullinated histone 3 (H3Cit), and net-like structure were performed. Vitreous samples were collected from patients with PDR; the PDR1 group had no need for repeated surgical intervention, and the PDR2 group had repeated vitreous bleeding or other complication and controls. Levels of MPO, H3Cit-MPO, and NE-MPO complex were measured with enzyme-linked immunosorbent assay (ELISA).
Results: Massive influx of CD11+ inflammatory cells, involving the anterior and posterior chambers, was observed in the murine eyes 24 h after the IL-8 or TNF-α injections. Cells excreted to their surroundings an extracellular net-like structure positive for NE, MPO, and H3Cit. H3Cit staining was abolished with the DNase I treatment, indicating the presence of extracellular DNA in the net-like structures. The vitreous samples of the patients with PDR2 contained statistically significantly higher levels of MPO (173±230) compared to those of the patients with PDR1 (12.0±33.0, $p<0.05$) or the controls (0.00, $p<0.01$). The levels of H3Cit-MPO and NE-MPO complexes were also statistically significantly higher in the patients with PDR2 (776.0±1274, 573.0±911.0, respectively) compared to those in the patients with PDR1 (0, $p<0.05$) and the controls (0, $p<0.05$).
Conclusions: This study showed the existence of NETosis in cytokine-induced ocular inflammation in a mouse model and human samples. Furthermore, the extent of NET complex formation was higher in a subset of patients who exhibited more complicated PDR.

In recent years, increasing evidence has suggested that inflammation plays a key role in the pathogenesis of a broad spectrum of ocular diseases [1]. Any process (including deregulated immune response) which alters retinal architecture, will have a devastating impact on vision [1].

Neutrophils play a major role in innate immunity, as they are the first responders at sites of infection [2]. Neutrophils are rapidly and extensively recruited from the blood circulation into the injured tissue, where they display a remarkable battery of toxic weapons. Until recently, it was known that neutrophils exert two main strategies when killing microorganisms: phagocytosis and degranulation [3]. Recently, a new strategy termed NETosis was revealed [4-9]. In this process, neutrophil extracellular trap (NET) structures arise from the release of the neutrophil's chromatin (mainly citrullinated histone) bound to specific granular proteins, such as neutrophil elastase (NE) and myeloperoxidase (MPO), thus entrapping microorganisms and amplifying microbial killing [4]. Recently, NETs were found to be implicated in the etiology of many inflammatory (non-infection) conditions, including systemic lupus erythematosus (SLE) [10], rheumatoid arthritis [11,12], and acute lung injury [13]. It is well documented that NETs can be formed in response to a variety of stimuli, including proinflammatory cytokines, such as IL-8 [5,8,14] and TNF-α [8,14]. In the eye, proinflammatory cytokines, such as IL-8 and TNF-α, were found to be involved in the pathogenesis of several ocular diseases, including diabetic retinopathy [15-17] and retinal vein occlusion [18,19]. However, the existence of NETosis in vitroretinal pathologies was not demonstrated.

In the present study, we aimed to assess the existence of NETosis in cytokine-induced ocular inflammation in a mouse model and human samples. We studied the involvement of

Correspondence to: Tami Livnat, Laboratory of Eye Research, Felsenstein Medical Research Center, Beilinson Campus, PetachTikva, Israel 49100; Phone: +972-3-9376740; FAX: +972-3-9376104; email: tami.livnat@sheba.health.gov.il

NETs in ocular inflammation induced by inflammatory cytokines (IL-8 and TNF-α) in a mouse model. Furthermore, we evaluated (to the best of our knowledge) for the first time, the presence of NETs complexes in patients with proliferative diabetic retinopathy (PDR) and correlated them with the severity of the disease. The results encourage in-depth analyses of the implication of NETosis in the pathology of PDR, as well as other ocular diseases.

METHODS

Animals: Forty 8-week-old pigmented male C57BL/6J mice in two sequential experiments were used in this study. Animals were obtained (Harlan Biotech Israel Ltd., Jerusalem, Israel) and handled according to the recommendations of the ARVO Statement for the Use of Animals in Ophthalmic and Visual Research and the hospital's Institutional Animal Care and Use Committee.

Induction of ocular inflammation: Animals were anesthetized with intraperitoneal (IP) injection of ketamine 40 mg/kg and xylazine 10 mg/kg, and the pupils were dilated with topical administration of 0.8% tropicamide eyedrops. Intravitreal injections were performed under an operating microscope (Zeiss Opmi 6S Microscope; Carl Zeiss Microscopy GmbH, Oberkochen, Germany). A microsyringe (33-gauge; Hamilton syringe, Energy Way, Reno, NV) was placed intravitreally in the retrolental space of the eye, and 1 µl per mouse of interleukin-8 (IL-8; 100 ng/µl), (R&D Systems, Minneapolis, MN) or tumor necrosis factor alpha (TNF-α; R&D Systems; 50 ng/µl) was injected. The control group was injected with sterile saline in a similar manner.

Histology: At each time point (n=5/group), animals were euthanized with carbon dioxide, and the eyes were enucleated. The eyes were fixed in 4% paraformaldehyde (PFA) in PBS (Dissolve 1 tablet in 200 ml water to obtain a 137 mM NaCl, 2.7 mM KCl and 10 mM phosphate buffer solution, pH 7.4 at 25 °C) for 1 h, dehydrated by increasing the sucrose gradient (5%, 10%, 20%, and 30%, 30 min to 1 h each), and cryopreserved in optimum cutting temperature (OCT; Thermo Fisher Scientific, Grand Island, NY). Serial 10-µm cryosections parallel to the optic nerve axis were obtained and stained with hematoxylin and eosin (H&E; American MasterTech Scientific, Lodi, CA). For histopathologic evaluation, the anterior and posterior chambers were examined under light microscopy (Olympus Optical Co., Tokyo, Japan).

Antibodies: The primary antibodies used in this study were rabbit polyclonal NE (Abcam, Cambridge, MA, 1:100), fluorescein isothiocyanate (FITC)-conjugated mouse monoclonal to MPO (Abcam, 1:200), rabbit polyclonal citrulline histone 3 (H3Cit; Abcam, 1:100), rat monoclonal CD11b (Abcam, 1:100), and rat monoclonal Ly6G (Abcam, 1:100). Secondary antibodies against the primary antibodies were donkey anti-rabbit AlexaFluor 568 (Invitrogen, Grand Island NY, NY, 1:500), donkey anti-rabbit 647 (Abcam, 1:200), donkey anti-rat 488 (Abcam, 1:500), and donkey anti-rat AlexaFluor 568 (Abcam, 1:500), respectively. Matched isotype controls were used as internal controls.

Immunofluorescence: A multistep staining protocol was designed based on the characteristics of the primary antibodies used. Briefly, the slides were hydrated, permeabilized with 0.5% TritonX-100 in PBS for 10 min, followed by blocking with either 10% goat or donkey antiserum in PBS (depending on the secondary antibody used) for 1 h. Thereafter, the slides were washed several times and incubated with the primary antibody in blocking solution for 1 h at room temperature. Tissue sections were then rinsed several times with PBS and incubated for 1 h at room temperature with a secondary antibody against the respective primary antibody. A similar procedure was followed for all antibodies in a sequence procedure. Then the slides were rinsed, and the cell nuclei were counterstained with 4',6-diamidino-2-phenylindole (DAPI; Invitrogen, 2 drops/ml according to the manufacturer's protocol), mounted with mounting medium (ProLong™ Gold Antifade mountant, Invitrogen, Grand Island, NY), and images were captured digitally using the Axio Imager Apotome microscope (Zeiss, Göttingen, Germany). A minimum of 20 fields at 63X magnification per case was used to evaluate for the presence of neutrophils (CD11b). Similarly, the presence of NE/MPO/H3Cit triple staining in which nuclear morphology and NETs were determined.

DNase I treatment: Consecutive cryosections positive for NETs were hydrated, permeabilized, and either left untreated or subjected to digestion with DNase I (Abcam) by 20 U/ml for 30 min at 37 °C. Thereafter, the slides were washed and stained for H3Cit using the immunofluorescence protocol mentioned above.

Study population: The study was approved by the Rabin Medical Center Institutional review board and adhered to the tenets of the Declaration of Helsinki and ARVO statement on human subjects and was approved by the Ethics Committee. The study was approved by the institutional review board; all patients provided written informed consent before the procedure. The study included 24 patients who underwent pars plana vitrectomy during 2013–2016. Patients were divided according to their pathology. Patients with PDR were divided into two groups: PDR1 (no need for repeated surgical intervention) and PDR2 (repeated vitreous bleeding or other complication). The control group (n=10) was composed of

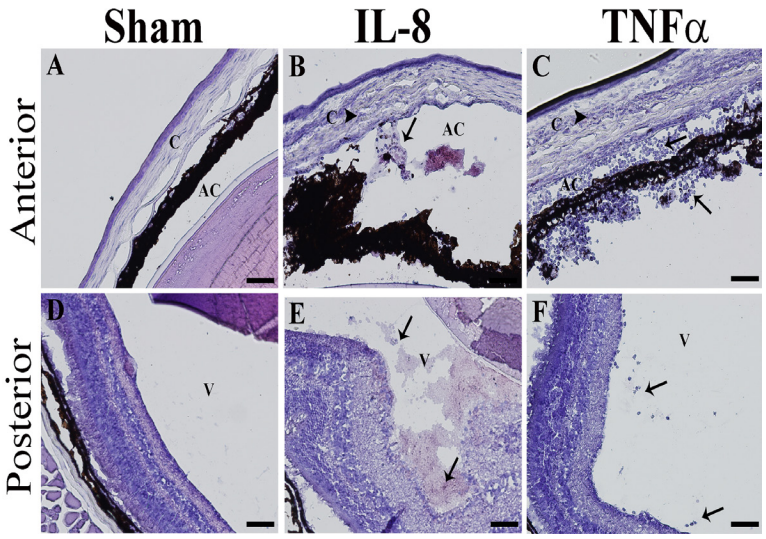

Figure 1. Histological evaluation of cytokine-induced ocular inflammation in the anterior and posterior chambers, respectively. **A**, **D**: Sham injected. **B**, **E**: Interleukin (IL)-8. **C**, **F**: Tumor necrosis factor alpha (TNF-α) 24 h post-injection. C = cornea; AC = anterior chamber; V = vitreous. Magnification = 10X. Scale bar = 100 µm.

patients with macular hole (MH) or epiretinal membrane (ERM). Exclusion criteria were age less than 18 years, previous vitrectomy, or combined cataract and pars plana vitrectomy. All patients underwent ophthalmic examination, and the medical and ocular history was recorded.

Sample collection: Vitreous samples were obtained via standard pars plana vitrectomy. During acquisition, infusion was set to air to prevent dilution. Samples were aliquoted (100 µl/vial) and stored at −80 °C pending laboratory analysis. No more than one freeze–thaw cycle was allowed before analysis.

Analyzing levels of MPO, H3Cit-MPO complex, and NE-MPO complex in the vitreous: MPO levels in the vitreous samples 100 µl/well (the samples were diluted 1:200 with a dilution buffer, R&D Systems) were measured using the Human MPO DuoSet enzyme-linked immunosorbent assay (ELISA) kit, according to the manufacturer's protocol (R&D Systems). MPO is present in extruded NET complexes mostly associated with H3Cit and NE. Such complexes were quantified with modified capture ELISA [11] In brief, a 96-well plate was precoated with human anti-H3Cit (Abcam, dilution 1:12,000) or human anti-NE antibodies (Abcam, dilution 1:12,000) overnight. The following day vitreous sample (diluted 1:200 with a dilution buffer, from the MPO DuoSet ELISA kit, R&D Systems) after which the MPO-associated complexes were detected using the human MPO ELISA kit, according to the manufacturer's protocol (R&D Systems).

Statistical analysis: A descriptive statistic was calculated for each marker. MPO, H3CitH3, and NE-MPO levels were compared between groups using linear transformation and one-way ANOVA (SPSS software). Least significant difference post hoc analysis was conducted to evaluate the significance of differences between groups. A p value of less than 0.05 was considered statistically significant, and a p value of less than 0.01 was considered statistically highly significant.

RESULTS

Histopathology: Histopathological analyses were conducted to evaluate cellular infiltration upon stimulation. Figure 1 is a representative image of three consecutive experiments with five animals per group. The sham-injected eyes presented with clear anterior and posterior chambers devoid of infiltrating immune cells (Figure 1A,D). IL-8 (Figure 1B,E) and TNF-α (Figure 1C,F) induced massive cellular infiltration, ranging in size and shape, into the anterior and posterior chambers (vitreous body), respectively. Cell infiltration was seen in the anterior chamber (arrows) and cornea (arrowheads), as well as in the ciliary body and the iris (data not shown). In the posterior chamber, cellular infiltration was seen in the vitreous body (Figure 1E,F, arrows) along with retinal folding, disorganization of the sensory layers, as well as retinal gliosis (data not shown; Figure 1).

Cellular infiltration: As neutrophils are the first responders at sites of infection [2] and play a key role in NETosis [4], we evaluated eyes injected with IL-8 and TNF-α for their presence, using the CD11b marker. The sham-injected eyes were negative for CD11b+ cells in the anterior and posterior chambers (Figure 2A,D, respectively). Massive infiltration of CD11b+ cells was observed in the anterior chamber and the vitreous (the posterior chamber) of the eyes injected with IL-8 (Figure 2B,E) and TNF-α (Figure 2C,F), respectively. The presence of CD11b-positive cells is consistent with

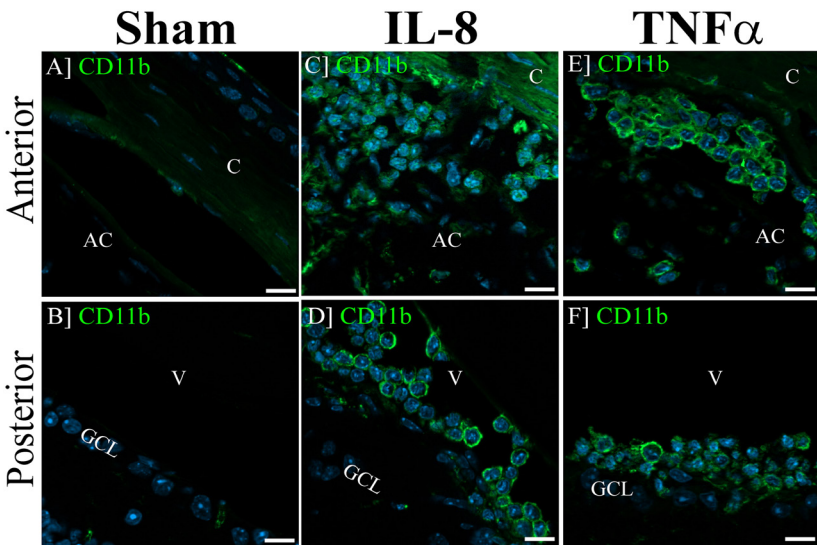

Figure 2. Neutrophils infiltration into the anterior and posterior chambers of the eye. Sham-injected (**A**, **D**), interleukin (IL)-8 (**B**, **E**) and tumor necrosis factor alpha (TNF-α) (**C**, **F**), 24 h post-injection. No cellular infiltration was observed in the sham-injected eyes (**A**, **E**) while abundant CD11b+ cells were seen in the eyes injected with IL-8 (**B**, **E**), and TNF-α (**C**, **F**). C= cornea; AC = anterior chamber; V = vitreous; GCL = ganglion cell layer. The results show representative images observed in five eyes (n=5/group). Magnification = 63X. Scale bar = 20 µm.

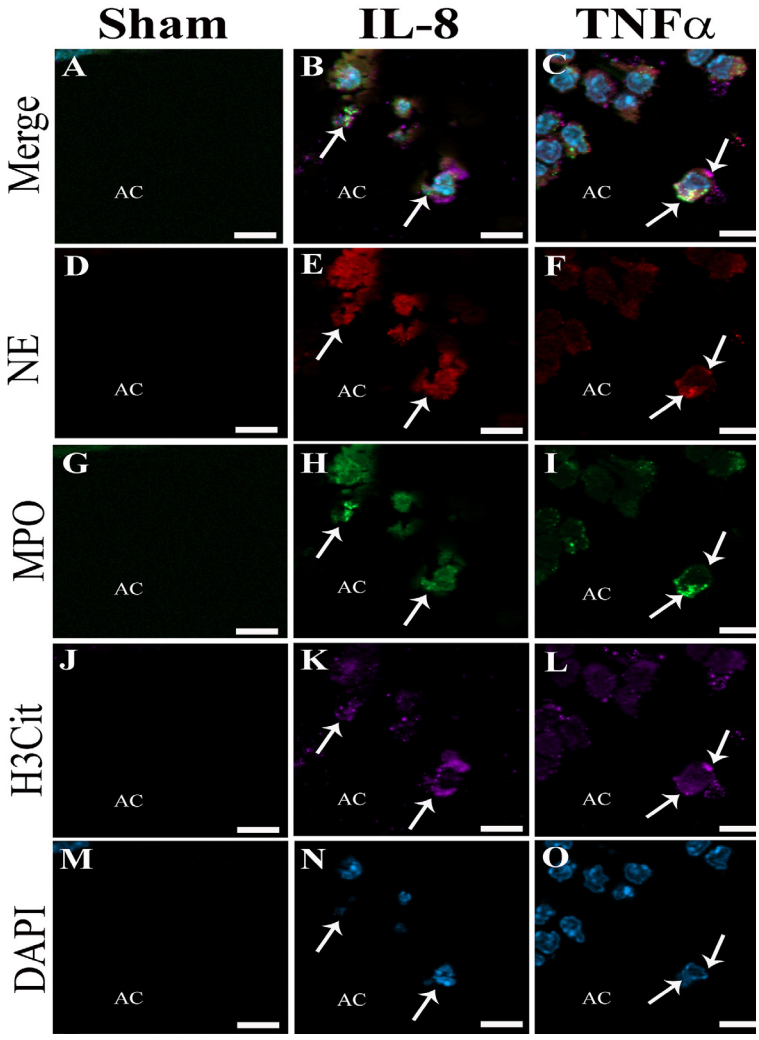

Figure 3. NET analysis in the anterior chamber upon IL-8 or TNF-α injections. The sham-injected eyes were negative for neutrophil extracellular traps (NETs; **A**, **D**, **G**, **J**, **M**). Netting neutrophils and NETs were observed in the eyes injected with interleukin (IL)-8 and tumor necrosis factor alpha (TNF-α) and were based on colocalization of neutrophil elastase (NE, red; **E**, **F**, arrows), myeloperoxidase (MPO, green; H, **I**, arrows), and H3Cit (purple; **K**, **L**, arrows). 4',6-diamidino-2-phenylindole (DAPI, blue; **N**, **O**, arrows) shows the nuclear morphology. Magnification = 63X. Scale bar = 50 µm.

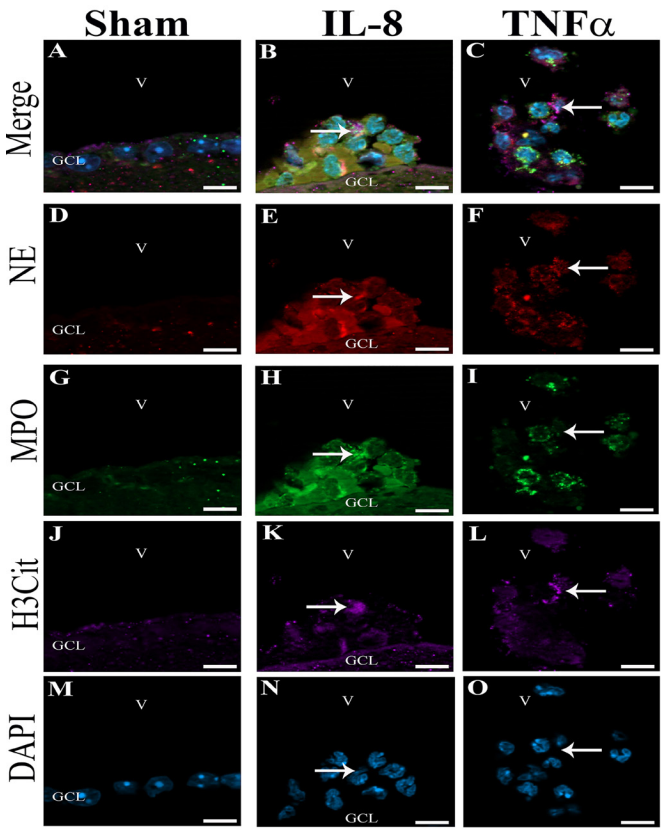

Figure 4. NET analysis in the posterior chamber upon IL-8 or TNF-α injections. The sham-injected eyes were negative for neutrophil extracellular traps (NETs; **A**, **D**, **G**, **J**, **M**). Netting neutrophils and NETs were observed in the eyes injected with interleukin (IL)-8 and tumor necrosis factor alpha (TNF-α) and were based on colocalization of neutrophil elastase (NE, red; **E**, **F**, arrows), myeloperoxidase (MPO, green; **H**, **I**, arrows), and citrullinated histone 3 (H3Cit, purple; **K**, **L**, arrows). 4',6-diamidino-2-phenylindole (DAPI, blue; **N**, **O**, arrows) shows the nuclear morphology. Magnification = 63X. Scale bar = 50 µm.

the histopathology results shown in Figure 1. Neutrophils were further validated with costaining for Ly6G and CD11b (Appendix 1) and defined by the classic polymorphonuclear granulocyte morphology (Appendix 2; Figure 2).

NET production by infiltrating neutrophils: We then asked the question whether the infiltrating neutrophils were associated with NETs formation. Eyes were examined for the presence of specific NET markers by triple-staining for NE (red), MPO (green), and H3Cit (purple) at different time points. NET complexes were found only at 24 h post-injection. Figure 3 and Figure 4 are representative images of the anterior and posterior chambers, respectively. The sham-injected eyes were neutrophil-free and negative for all three markers (Figure 3 and Figure 4A,D,G,J,M). Netting neutrophils were found in the anterior and posterior chambers of the eyes injected with IL-8 and TNF-α and were based on costaining of NE (red; Figure 3, Figure 4E,F; arrows), MPO (green; Figure 3, Figure 4H,I; arrows), and H3Cit (purple; Figure 3, Figure 4K,L, arrows). DAPI (blue; Figure 3, Figure 4N,O, arrows) shows the nuclear morphology. Both cytokines were accompanied by many NET loci, associated with very strong staining of citrullinated histones (purple). NETosis was particularly pronounced in areas of aggregated neutrophils

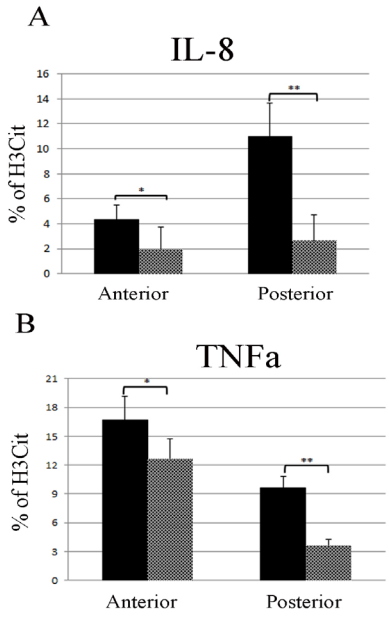

Figure 5. The effect of DNase I treatment on extracellular citrullinated DNA. Number of citrullinated histone 3 (H3Cit) loci with and without DNase I treatment in the anterior and posterior chambers of interleukin (IL)-8 (**A**) and tumor necrosis factor alpha (TNF-α) (**B**). *Statistically significant; p<0.05, ** highly significant, p<0.001.

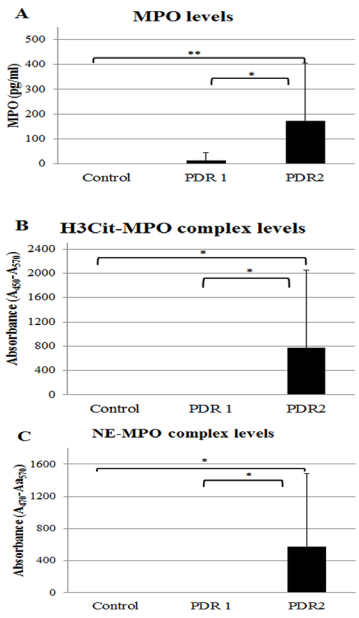

Figure 6. Vitreous levels of NET complexes found in patients with PDR. Myeloperoxidase (MPO) (**A**), citrullinated histone 3-myeloperoxidase (H3Cit-MPO) complex (**B**), and neutrophil elastase-myeloperoxidase (NE-MPO) complex (**C**). PDR = proliferative diabetic retinopathy; PDR1 = had no need for repeated surgical intervention; PDR2 = had repeated vitreous bleeding or other complication. *Statistically significant; p<0.05, **, highly statistically significant, p<0.01.

Table 1. PDR patients' demographic and clinical characteristics.

Variable	Control	PDR1	PDR2
Patients	n=10	n=7	n=5
Age	68±9	58±11	44±8
Gender (F/M)	5/5	1/6	1/4
Diabetes (yes/no)	2/8	6/0	6/0
Hypertention (yes/no)	5/2	3/4	2/3
Smoking	n/a	n/a	n/a
Operated eye (R/L)	5/5	2/5	3/2
VH (yes/no)	0/10	5/2	4/1
TRD (yes/no)	n/a	2/5	1/4
Glaucoma (yes/no)	2/8	2/5	1/4
AMD (yes/no)	1/8	0/7	0/5
Avastin pre-treatment (yes/no)	0/8	5/2	2/3
HBA1C	n/a	8.8±1	9.8±3

Control (includes MH, macular holes; ERM, epiretinal membrane); PDR, proliferative diabetic retinopathy; PDR1- with no need for repeated surgical intervention; PDR2- with repeated vitreous bleeding or other complication.

and was manifested by the extracellular colocalization of all the three markers as shown in the merged images (Figure 3, Figure 4B,C). Isotype controls were used as internal controls (Appendix 3). No significant difference was found for the time period of NET clearance between the anterior and posterior chambers.

NET degradation with DNase I treatment: We confirmed the presence of extracellular DNA in the NETs using DNase I treatment followed by immunostaining for citrullinated histone. Figure 5A,B illustrate the decrease in the number of H3Cit loci for IL-8 and TNF-α, respectively. The sham-injected eyes were negative for H3Cit staining indicating the absence of the NETs ex vivo treatment with DNase exerted no effect in these samples (Appendix 4 and Appendix 5). IL-8 and TNF-α were associated with infiltrated cells surrounded by extruded DNA (indicated by the H3Cit-positive staining) in the anterior and posterior chambers (Figure 5A,B, black bars). DNase I treatment induced a significant degradation of DNA, leaving fade traces of H3Cit (Figure 5A,B, gray bars, $p<0.05$ and $p<0.001$, anterior and posterior chambers, respectively).

Evaluation of NETs complexes in vitreous samples of patients with PDR: We evaluated the generation of NET components, such as MPO, H3-CitH3, and NE-MPO complexes, in the vitreous of patients with PDR. The demographic and clinical characteristics of the patients with PDR are summarized in Table 1.

The patients were divided into two groups based on the severity of PDR [20]: The PDR1 group had no need for repeated surgical intervention, and the PDR2 group had repeated vitreous bleeding or other complication. The results are summarized in Figure 6. We found that patients with PDR2 exhibited significantly higher levels of MPO (Figure 6A; 173±230) compared to the patients with PDR1 (Figure 6A; 12±33, *$p<0.05$) or the controls (Figure 6A; 0, **$p<0.01$). The levels of H3Cit-MPO and NE-MPO complexes were also statistically significantly higher in the patients with PDR2 (Figure 6B; 776.0±1274, Figure 6C; 573±911, respectively) compared to those in the patients with PDR1 (Figure 6B,C; 0, *$p<0.05$) and the controls (Figure 6B,C; 0, *$p<0.05$).

DISCUSSION

NETosis, the process of neutrophil cell death involving release of nuclear chromatin followed by the formation of extracellular DNA traps, is an important mechanism of immune defense in response to various stimuli [4,5]. In this study, we used a mouse model of intraocular inflammation to demonstrate the occurrence of NETosis and to characterize the mechanism of this process. We found that inflammatory

cytokines induce NET formation: We showed the appearance of NET-forming neutrophils following the injection of IL-8 and TNF-α into murine eyes. The results demonstrated that inflammatory mediators provoked an intense influx of inflammatory cells, especially neutrophils (CD11b+), into the anterior and posterior chambers with the appearance of NET structures and proteins. Formation of NETs was demonstrated by the presence of specific NET markers, based on triple-staining for MPO, NE, and H3Cit. Formation of NETs was further supported by the observation of reduction of H3Cit staining upon DNase I treatment.

Retinal abnormalities may affect vision and potentially induce vision loss. The cytokines used in this study (IL-8 and TNF-α) secreted by different retinal cells are often associated with the disruption of macro- and microvessels (induce retinal neovascularization), ocular inflammation (uvea), activation of nuclear factor kappa beta, apoptosis of retinal ganglion cells, as well as activation of metalloproteases [21,22]. All these processes may affect different layers of the retina and thus, vision. In addition to the signal transduction pathways activated by IL-8 and TNF-α, these cytokines are known to induce infiltration of different immune cells, predominantly neutrophils but also macrophages, monocytes, and T cells. Infiltrating immune cells are known to secrete more cytokines and interact with different retinal cells and integrins. Uncontrolled activation, interaction with retinal macrophages, and secretion of different cytokines are all associated with retinal pathogenesis and vision loss. Direct treatment with either anti-IL-8 or anti-TNF-α agents (for wet age-related macular degeneration) in the clinical setting has been suggested; however, concerns have been raised in view of the importance of these cytokines in normal immune response in the eye, which may be impaired by their complete inhibition [21,22].

Much of the cytotoxic effect of NETs is attributed to the extracellular histones which prevent the degradation of extruded DNA. It was confirmed that extracellular histones contribute to tissue injury and microvascular complications associated with sepsis and small vessel vasculitis [8,23-31]. Evidence from diabetic patients showed NETosis halts the healing and repair of diabetic foot ulcers [32-35]. Recently, histones were found in the vitreous of patients who had retinal detachment [36,37], which may suggest formation of NETs in this condition.

DNase administration for the degradation of extracellular DNA (Pulmozyme®) has been approved by the U.S. Food and Drug Administration for treatment of cystic fibrosis [38,39]. Tibrewal et al. demonstrated that treatment of patients with dry eye disease found to be associated with NETosis with recombinant human DNase I eye drops resulted in symptomatic improvement [40]. Thus, the present results showing the appearance of NETs in response to inflammatory stimulus, along with their disappearance following degradation of extracellular citrullinated DNA by DNase, strongly suggest that NETs are involved in ocular inflammatory diseases and may also potentially offer a new therapeutic approach for the treatment of such diseases.

Interestingly, citrullinated DNA was also found in some areas of the retina (IL-8, Appendix 5), which may be related to gliosis [41]. Therefore, DNase treatment may not only alleviate NETs complexes in the vitreous but also prevent side effects associated with cytokine elevation, such as gliosis.

Although NETosis plays an important role in the destruction of pathogens, it may also be involved in pathological inflammatory conditions that occur in the absence of infectious microorganisms [2]. Accumulation and subsequent activation of neutrophils are central events mediating the inflammatory response. Increasing evidence supports the important role of cytokines (such as IL-8 and TNF-α) and neutrophil-mediated inflammation in the pathogenesis of many ocular diseases, including diabetic retinopathy [15-17,42-44], retinal vein occlusion [18,19,45,46], as well as age-related macular degeneration [1,47-49], retinitis pigmentosa [50], dry eye disease [51,52], and keratoconus [53,54]. The present study showed the ability of two major cytokines (IL-8 and TNF-α) to induce NETs in a controlled mouse model of ocular inflammation. Potential association between these and other cytokines with NETosis in human ocular pathologies should be further investigated. To date, the presence of NETs in the eye has been reported only in patients with dry eye disease [37,55], and no other observations have been attributed to NETosis in the context of intraocular diseases.

In this study, we showed, to the best of our knowledge, for the first time, the existence of NET-associated proteins in a small cohort of patients with complicated PDR. The exact role of NETosis in the etiology of PDR is currently unknown, thus encouraging in-depth studies to evaluate this aspect in patients with PDR and other inflammatory ocular diseases. Such studies may shed more light on the pathophysiological mechanisms of PDR, along with opening a pathway to the development of novel therapeutic strategies based on inhibition of NETosis.

Neutrophil validation: We evaluated the eyes injected with IL-8 and TNF-α for their presence, using the CD11b/Ly6G markers. The sham-injected eyes were negative for CD11b/Ly6G cells in both posterior chambers (Appendix 1). Massive infiltration of CD11b/Ly6G cells was observed in the posterior chamber of the eyes injected with IL-8 and TNF-α (Appendix

1). The presence of Ly6G (Appendix 1) and CD11b (Appendix 1) positive cells is consistent with the histopathology results shown in Figure 1. Neutrophils were validated as defined by the classic polymorphonuclear granulocyte morphology (Appendix 2, DAPI staining, higher resolution).

Validation of NET production: Isotype control analysis: As NET production is the scope of this paper and authentication of the results was highly valuable, staining using isotype controls was conducted throughout the study for each of the antibodies and multiple sites of the anterior and posterior chambers. As can be seen, the donkey anti-rabbit Alexa-Fluor 568 had no non-specific staining at either the anterior or posterior chambers (Appendix 3, respectively). Minimal autofluorescence was observed when the donkey anti-rat 488 at both the anterior and posterior chambers (Appendix 3, respectively). No staining was observed for the donkey anti-rabbit 647 isotype control (Appendix 3, anterior and posterior chambers, respectively). DAPI nuclear staining was used as an internal control for neutrophil validation and localization (Appendix 3, arrows).

NET degradation by DNase I treatment: The presence of extracellular DNA in the NETs was evaluated using DNase I treatment followed by immunostaining for citrullinated histone. Appendix 4 and Appendix 5 are representative images of the anterior and posterior chambers, respectively. Sham-injected eyes were negative for H3Cit staining, indicating the absence of NETs (Appendix 4 and Appendix 5). Ex vivo treatment with DNase exerted no effect in these samples. IL-8 and TNF-α were associated with infiltrated cells surrounded by extruded DNA, as indicated by positive staining for H3Cit (purple; Appendix 4 and Appendix 5, arrows). Upon DNase I treatment, the majority of the DNA was degraded, leaving fade traces of H3Cit (Appendix 4 and Appendix 5, arrows). Interestingly, in the IL-8 group, the ganglion cell layer was also positive for H3Cit (Appendix 5), which may be related to retinal gliosis (see also histological section, Figure 1).

APPENDIX 1.

Validation of neutrophil infiltration. Neutrophils infiltration was demonstrated by staining with Ly6G (red; panels A, B) and CD11b (green; panels C, D); merge images with DAPI for nuclear staining (blue) is shown in panels E, F. The figure shows staining of sham injected (A, C, E) and IL-8/TNFα -injected (B, D, F) eyes. Ganglion cell layer (GCL), vitreous (V). Representative images of 3 eyes (n=3/group), magnification x63, scale bar 20 µm. To access the data, click or select the words "Appendix 1"

APPENDIX 2.

Neutrophils at higher resolution showing their classic polymorphonuclear granulocyte morphology. A] CD11b, B] DAPI and C] merge. Representative image x100, scale bar 10 µm. To access the data, click or select the words "Appendix 2"

APPENDIX 3.

Isotype control staining. A] donkey anti-rabbit AlexaFluor 568, B] donkey anti-rat AlexaFluor 488, C] donkey anti-rabbit AlexaFluor 647 and D] DAPI. Cornea (C), anterior chamber (AC), vitreous (V), nerve fiber layer (NFL), ganglion cell layer (GCL). Representative images of 3 eyes (n=3/group) for both IL-8 and TNFα at the anterior and posterior sections, respectively. Magnification x63, scale bar 20 µm. To access the data, click or select the words "Appendix 3"

APPENDIX 4.

The effect of DNase I treatment on extracellular citrullinated DNA in the anterior chamber. Sham injected eyes (A, D), IL-8 (B, E) and TNFα (C, F) injected eyes. Upon DNase I treatment, the majority of extracellular DNA (B, C, arrows) was digested (E, F, arrows). Cornea (C), anterior chamber (AC). Representative images of 3 eyes (n=3/group), magnification x63, scale bar 20µm. To access the data, click or select the words "Appendix 4"

APPENDIX 5.

The effect of DNase I treatment on extracellular citrullinated DNA in the posterior chamber. Sham injected eyes (A, D), IL-8 (B, E) and TNFα (C, F) injected eyes. Upon DNase I treatment, the majority of extracellular DNA (B, C, arrows) was digested (E, F, arrows). Ganglion cell layer (GCL), vitreous (V). Representative images of 3 eyes (n=3/group), magnification x63, scale bar 20µm. To access the data, click or select the words "Appendix 5"

ACKNOWLEDGMENTS

This study was supported by research grant of The Dr. Herman Schauder Research Fund: Sackler Faculty of Medicine, Tel-Aviv University. The Dr. Herman Schauder Research 376 Fund: Sackler Faculty of Medicine, Tel-Aviv University. Grant no. 0601242322.

REFERENCES

1. Whitcup SM, Nussenblatt RB, Lightman SL, Hollander DA. Inflammation in Retinal Disease. Int J Inflamm 2013; 2013:724648-[PMID: 24109539].

2. Nathan C. Neutrophils and immunity: challenges and opportunity. Nat Rev Immunol 2006; 6:173-82. [PMID: 16498448].

3. Zysk G, Bejo L, Schneider-Wald BK, Nau R, Heinz HP. Induction of necrosis and apoptosis of neutrophil granulocytes by Streptococcus pneumoniae. Clin Exp Immunol 2000; 122:61-6. [PMID: 11012619].

4. Brinkmann V, Reichard U, Goosmann C, Fauler B, Uhlemann Y, Weiss DS, Weinrauch Y, Zychlinsky A. Neutrophil extracellular traps kill bacteria. Science 2004; 303:1532-5. [PMID: 15001782].

5. Fuchs TA, Abed U, Goosmann C, Hurwitz R, Schulze I, Wahn V, Weinrauch Y, Brinkmann V, Zychlinsky A. Novel cell death program leads to neutrophil extracellular traps. J Cell Biol. 2007 15;176(2):231–241.

6. Kolacskowska E, Kubes P. Neutrophil recruitment and function in health and inflammation. Nat Rev Immunol 2013; 13:159-75. [PMID: 23435331].

7. Neeli I, Kahan SN, Radic M. Histone demination as a response to inflammatory stimuli in neutrophils. J Immunol 2008; 180:1895-902. [PMID: 18209087].

8. Remijsen Q, Kuijpers TW, Wirawan E, Lippens S, Vandenabeele P, Vanden Berghe T. Dying for a cause: NETosis, mechanisms behind an antimicrobial cell death modality. Cell Death Differ 2011; 18:581-8. [PMID: 21293492].

9. Yipp BG, Petri B, Salina D, Jenne CN, Scott BN, Zbytnuik LD, Pittman K, Asaduzzaman M, Wu K, Meijndert HC, Malawista SE, de Boisfleury Chevance A, Zhang K, Conly J, Kubes P. Infection-induced NETosis is a dynamic process involving neutrophil multitasking in vivo. Nat Med 2012; 18:1386-93. [PMID: 22922410].

10. Gina S. Garcia-Romo, Simone Caielli, Barbara Vega, John Connolly, Florence Allantaz, Zhaohui Xu, Marilynn Punaro, Jeanine Baisch, Cristiana Guiducci, Robert L. Coffman, Franck J. Barrat, Jacques Banchereau, and Virginia Pascual. Netting neutrophils are major inducers of type I IFN production in pediatric systemic lupus erythematosus. Sci Transl Med 2011; 3:73ra20-[PMID: 21389264].

11. Chowdhury CS, Giaglis S, Walker UA, Buser A, Hahn S, Hasler P. Enhanced neutrophil extracellular trap generation in rheumatoid arthritis: analysis of underlying signal transduction pathways and potential diagnostic utility. Arthritis Res Ther 2014; 16:R122-[PMID: 24928093].

12. Khandpur R, Carmona-Rivera C, Vivekanandan-Giri A, Gizinski A, Yalavarthi S, Knight JS, Friday S, Li S, Patel RM, Subramanian V, Thompson P, Chen P, Fox DA, Pennathur S, Kaplan MJ. NETs are a source of citrullinated autoantigens and stimulate inflammatory responses in rheumatoid arthritis. Sci Transl Med 2013; 5:178ra40-[PMID: 23536012].

13. Thomas GM, Carbo C, Curtis BR, Martinod K, Mazo IB, Schatzberg D, Cifuni SM, Fuchs TA, von Andrian UH, Hartwig JH, Aster RH, Wagner DD. Extracellular. DNA traps are associated with the pathogenesis of TRALI in humans and mice. Blood 2012; 119:6335-43. [PMID: 22596262].

14. . Keshari RS1. Jyoti A, Dubey M, Kothari N, Kohli M, Bogra J, Barthwal MK, Dikshit M. Cytokines induced neutrophil extracellular traps formation: implication for the inflammatory disease condition. PLoS One 2012; 7:e48111-[PMID: 23110185].

15. Zhou L, Wang S, Xia X. Role of intravitreal inflammatory cytokines and angiogenic factors in proliferative diabetic retinopathy. Curr Eye Res 2012; 37:416-20. [PMID: 22409294].

16. Takeuchi M, Sato T, Tanaka A, Muraoka T, Taguchi M, Sakurai Y, Karasawa Y, Ito M. Elevated Levels of Cytokines Associated with Th2 and Th17 Cells in Vitreous Fluid of Proliferative Diabetic Retinopathy Patients. PLoS One 2015; 10:e0137358-[PMID: 26352837].

17. Rangasamy S, McGuire PG, Das A. Diabetic retinopathy and inflammation: novel therapeutic targets. Middle East Afr J Ophthalmol 2012; 19:52-9. [PMID: 22346115].

18. Fonollosa A, Garcia-Arumi J, Santos E, Macia C, Fernandez P, Segura RM, Zapata MA, Rodriguez-Infante R, Boixadera A, Martinez-Castillo V. Vitreous levels of interleukine-8 and monocyte chemoattractant protein-1 in macular oedema with branch retinal vein occlusion. Eye (Lond) 2010; 24:1284-90. [PMID: 20111061].

19. Jung SH, Kim KA, Sohn SW, Yang SJ. Association of aqueous humor cytokines with the development of retinal ischemia and recurrent macular edema in retinal vein occlusion. Invest Ophthalmol Vis Sci 2014; 55:2290-6. [PMID: 24398091].

20. Rusnak S, Vrzalova J, Sobotova M, Hecova L, Ricarova R, Topolcan O. The Measurement of Intraocular Biomarkers in Various Stages of Proliferative Diabetic Retinopathy Using Multiplex xMAP Technology. J Ophthalmol 2015; 2015:424783-[PMID: 26491551].

21. Ghasemi H, Ghazanfari T, Yaraee R, Faghihzadeh S, Hassan ZM. Roles of IL-8 in ocular inflammations: a review. Ocul Immunol Inflamm 2011; 19:401-12. [PMID: 22106907].

22. Al-Gayyar MM, Elsherbiny NM. Contribution of TNF-α to the development of retinal neurodegenerative disorders. Eur Cytokine Netw 2013; 24:27-36. [PMID: 23608634].

23. Martinod K, Wagner DD. Thrombosis: tangled up in NETs. Blood 2014; 123:2768-76. [PMID: 24366358].

24. Kessenbrock K, Krumbholz M, Schönermarck U, Back W, Gross WL, Werb Z, Gröne HJ, Brinkmann V, Jenne DE. Netting neutrophils in autoimmune small-vessel vasculitis. Nat Med 2009; 15:623-5. [PMID: 19448636].

25. Yu Y, Su K. Neutrophil Extracellular Traps and Systemic Lupus Erythematosus. J Clin Cell Immunol 2013; 4:139-[PMID: 24244889].

26. Hakkim A, Fürnrohr BG, Amann K, Laube B, Abed UA, Brinkmann V, Herrmann M, Voll RE, Zychlinsky A. Impairment of neutrophil extracellular trap degradation is associated with lupus nephritis. Proc Natl Acad Sci USA 2010; 107:9813-8. [PMID: 20439745].

27. Dwivedi N, Radic M. Citrullination of autoantigens implicates NETosis in the induction of autoimmunity. Ann Rheum Dis 2014; 73:483-91. [PMID: 24291655].

28. Kaplan MJ, Radic M. Neutrophil extracellular traps: double-edged swords of innate immunity. J Immunol 2012; 189:2689-95. [PMID: 22956760].

29. Brinkmann V, Zychlinsky A. Beneficial suicide: why neutrophils die to make NETs. Nat Rev Microbiol 2007; 5:577-782. [PMID: 17632569].

30. Branzk N, Papayannopoulos V. Molecular mechanisms regulating NETosis in infection and disease. Semin Immunopathol 2013; 35:513-30. [PMID: 23732507].

31. Almyroudis NG, Grimm MJ, Davidson BA, Röhm M, Urban CF, Segal BH. NETosis and NADPH oxidase: at the intersection of host defense, inflammation, and injury. Front Immunol 2013; 4:45-[PMID: 23459634].

32. Fadini GP, Menegazzo L, Rigato M, Scattolini V, Poncina N, Bruttocao A, Ciciliot S, Mammano F, Ciubotaru CD, Brocco E, Marescotti MC, Cappellari R, Arrigoni G, Millioni R, Vigili de Kreutzenberg S, Albiero M, Avogaro A. NETosis Delays Diabetic Wound Healing in Mice and Humans. Diabetes 2016; a65:1061-71. [PMID: 26740598].

33. Fadini GP, Menegazzo L, Scattolini V, Gintoli M, Albiero M, Avogaro A. A perspective on NETosis in diabetes and cardiometabolic disorders. Nutr Metab Cardiovasc Dis 2016; b26:1-8. [PMID: 26719220].

34. Wong SL, Demers M, Martinod K, Gallant M, Wang Y, Goldfine AB, Kahn CR, Wagner DD. Diabetes primes neutrophils to undergo NETosis, which impairs wound healing. Nat Med 2015; 21:815-9. [PMID: 26076037].

35. Menegazzo L, Ciciliot S, Poncina N, Mazzucato M, Persano M, Bonora B, Albiero M, Vigili de Kreutzenberg S, Avogaro A, Fadini GP. NETosis is induced by high glucose and associated with type 2 diabetes. Acta Diabetol 2015; 52:497-503. [PMID: 25387570].

36. Kawano H, Ito T, Yamada S, Hashiguchi T, Maruyama I, Hisatomi T, Nakamura M, Sakamoto T. Toxic effects of extracellular histones and their neutralization by vitreous in retinal detachment. Lab Invest 2014; a94:569-85. [PMID: 24614198].

37. Kawano H, Sakamoto T, Ito T, Miyata K, Hashiguchi T, Maruyama I. Hyaluronan protection of corneal endothelial cells against extracellular histones after phacoemulsification. J Cataract Refract Surg 2014; b40:1885-93. [PMID: 25442884].

38. Konstan MW, Wagener JS, Pasta DJ, Millar SJ, Jacobs JR, Yegin A, Morgan WJ. Scientific Advisory Group and Investigators and Coordinators of Epidemiologic Study of Cystic Fibrosis. Clinical use of dornase alpha is associated with a slower rate of FEV1 decline in cystic fibrosis. Pediatr Pulmonol 2011; 46:545-53. [PMID: 21438174].

39. Rahman S, Gadjeva M. Does NETosis Contribute to the Bacterial Pathoadaptation in Cystic Fibrosis? Front Immunol 2014; 5:378-[PMID: 25157250].

40. Tibrewal S, Ivanir Y, Sarkar J, Nayeb-Hashemi N, Bouchard CS, Kim E, Jain S. Hyperosmolar stress induces neutrophil extracellular trap formation: implications for dry eye disease. Invest Ophthalmol Vis Sci 2014; 55:7961-9. [PMID: 25406284].

41. Wizeman JW, Mohan R. Expression of peptidylarginine deiminase 4 in an alkali injury model of retinal gliosis. Biochem Biophys Res Commun 2017; 487:134-9. [PMID: 28400047].

42. Kim SY, Johnson MA, McLeod DS, Alexander T, Hansen BC, Lutty GA. Neutrophils are associated with capillary closure in spontaneously diabetic monkey retinas. Diabetes 2005; 54:1534-42. [PMID: 15855343].

43. Joussen AM, Poulaki V, Le ML, Koizumi K, Esser C, Janicki H, Schraermeyer U, Kociok N, Fauser S, Kirchhof B, Kern TS, Adamis AP. A central role for inflammation in the pathogenesis of diabetic retinopathy. FASEB J 2004; 18:1450-2. [PMID: 15231732].

44. Woo SJ, Ahn SJ, Ahn J, Park KH, Lee K. Elevated systemic neutrophil count in diabetic retinopathy and diabetes: a hospital-based cross-sectional study of 30,793 Korean subjects. Invest Ophthalmol Vis Sci 2011; 52:7697-703. .

45. Ehlers JP, Fekrat S. Retinal vein occlusion: beyond the acute event. Surv Ophthalmol 2011; 56:281-99. [PMID: 21601903].

46. Zapponi KC, Mazetto BM, Bittar LF, Barnabé A, Santiago-Bassora FD, De Paula EV, Orsi FA, Franco-Penteado CF, Conran N, Annichino-Bizzacchi JM. Increased adhesive properties of neutrophils and inflammatory markers in venous thromboembolism patients with residual vein occlusion and high D-dimer levels. Thromb Res 2014; 133:736-42. [PMID: 24560897].

47. Buschini E, Piras A, Nuzzi R, Vercelli A. Age related macular degeneration and drusen: neuroinflammation in the retina. Prog Neurobiol 2011; 95:14-25. [PMID: 21740956].

48. Cascella R, Ragazzo M, Strafella C, Missiroli F, Borgiani P, Angelucci F, Marsella LT, Cusumano A, Novelli G, Ricci F, Giardina E. Age-related macular degeneration: insights into inflammatory genes. J Ophthalmol 2014; 2014:582842-[PMID: 25478207].

49. Kauppinen A, Paterno JJ, Blasiak J, Salminen A, Kaarniranta K. Inflammation and its role in age-related macular degeneration. Cell Mol Life Sci 2016; 73:1765-86. [PMID: 26852158].

50. Yoshida N, Ikeda Y, Notomi S, Ishikawa K, Murakami Y, Hisatomi T, Enaida H, Ishibashi T. Clinical evidence of sustained chronic inflammatory reaction in retinitis pigmentosa. Ophthalmology 2013; 120:100-5. [PMID: 22986109].

51. Stevenson W, Chauhan SK, Dana R. Dry eye disease: an immune-mediated ocular surface disorder. Arch Ophthalmol 2012; 130:90-100. [PMID: 22232476].

52. Dionne K, Redfern RL, Nichols JJ, Nichols KK. Analysis of tear inflammatory mediators: A comparison between the microarray and Luminex methods. Mol Vis 2016; 22:177-88. [PMID: 26957901].

53. Galvis V, Sherwin T, Tello A, Merayo J, Barrera R, Acera A. Keratoconus: an inflammatory disorder? Eye (Lond) 2015; 29:843-59. [PMID: 25931166].

54. Wisse RP, Kuiper JJ, Gans R, Imhof S, Radstake TR, Van der Lelij A. Cytokine Expression in Keratoconus and its Corneal Microenvironment: A Systematic Review. Ocul Surf 2015; 13:272-83. [PMID: 26235733].

55. Sonawane S, Khanolkar V, Namavari A, Chaudhary S, Gandhi S, Tibrewal S, Jassim SH, Shaheen B, Hallak J, Horner JH, Newcomb M, Sarkar J, Jain S. Ocular surface extracellular DNA and nuclease activity imbalance: a new paradigm for inflammation in dry eye disease. Invest Ophthalmol Vis Sci 2012; 53:8253-63. [PMID: 23169882].

Articles are provided courtesy of Emory University and the Zhongshan Ophthalmic Center, Sun Yat-sen University, P.R. China. The print version of this article was created on 13 December 2017. This reflects all typographical corrections and errata to the article through that date. Details of any changes may be found in the online version of the article.